

TTYH3, a potential prognosis biomarker associated with immune infiltration and immunotherapy response in lung cancer

Zimeng Wei

Wuhan University

Xingruo Zeng

Wuhan University

Yufei Lei

Wuhan University

Hengjing He

Wuhan University

Muhammad Jamal

Wuhan University

Chengjie Zhang

Wuhan University

Haiyan Tan

Renmin Hospital of Wuhan University

Songping Xie

Renmin Hospital of Wuhan University

Qiuping Zhang (✉ qpzhang@whu.edu.cn)


Wuhan University

Research Article

Keywords: Lung cancer, TTYH3, Biomarker, Proliferation, Immune infiltration, Immunotherapy response

Posted Date: April 28th, 2022

DOI: <https://doi.org/10.21203/rs.3.rs-1589897/v1>

License:  This work is licensed under a Creative Commons Attribution 4.0 International License. [Read Full License](#)

Abstract

Purpose

The recognition of new diagnostic and prognostic biological markers for lung cancer is an essential and eager study. It's shown that ion channels play important roles in regulating various cellular processes and have been suggested to be associated with patient survival. However, TTYH3, as a novel maxi-Cl⁻ channel, its role in lung cancer remains elusive.

Methods

The expression, diagnosis and prognostic efficacy of TTYH3 were analyzed by public databases and clinical samples. Cell functional experiments used to explore the effects of TTYH3 on cell ability. GO and KEGG enrichment analysis revealed pathway that TTYH3 and its co-expressed genes were enriched in. TIMER and R language analyses were used to detect the correlation between TTYH3 and immune cell infiltration and the immunotherapy response.

Results

TTYH3 was found up-regulated in lung cancer tissues compared to normal tissues and possessed a prominent diagnostic and prognostic value. Knockdown TTYH3 significantly inhibited the proliferation of lung cancer cells. Enrichment analyses results showed that TTYH3 and its co-expressed genes were mainly involved in immune related signaling pathways. Further investigation clarified that TTYH3 had a positive correlation with the infiltration of macrophage, T cell regulatory, CD4⁺ T cell and high TTYH3 expression indicated worse immunotherapy response and shorter survival after immune checkpoint blockade treatment.

Conclusion

This study not only deciphers the diagnostic and prognostic value of TTYH3 but also provides TTYH3-based estimation of immunotherapy response for lung cancer patients, which might provide new strategies like anti-TTYH3 combined with immune therapy for the treatment of lung cancer.

Introduction

Lung cancer is the leading cause of cancer-related morbidity and mortality globally¹. Despite a substantial progress achieved in cancer screening and personal therapy in recent years, the 5-year survival of lung cancer remains around 4–17% depending on stage and geographical differences and patients with early-stage lung cancer often encounter recurrences or distant metastases, which lead to the poor prognosis².

It has been confirmed that, except for tumor cells, there are many kinds of stromal cells such as mesenchymal cells, endothelial cells and immune cells surrounded in tumor microenvironment and the infiltration of immune cells is considered to be closely related to the poor prognosis of tumor^{3–5}. Indeed, assessing the infiltration extent of immune cell in the tumor microenvironment has proved to be an important complementary indicator for the

TNM system to predict tumor relapse and death⁶⁻⁸. The development of immunotherapy has drastically improved the prognosis of some patients. However, part of patients couldn't accomplish the expected positive responses to current immunotherapy³ and this largely depends on the molecular mechanism of interactions between infiltrating immune cells and cancer cells^{9,10}. Therefore, it is of great significance to find a target molecule that can comprehensively reflect the tumor cells and infiltration of immune cells for the diagnosis, treatment and prognosis of lung cancer.

The tweety family members (TTYHs) have been reported to encode the pore-forming subunits of the swelling-dependent volume-regulated anion channel¹¹, which is fundamental to the functions and survival of animal cells under physiological and pathological conditions¹². The TTYHs possesses 5 or 6 transmembrane segments encoding a large conductance Cl⁻-channel¹³. TTYH1 plays an indispensable role during mitosis in early embryogenesis, possibly by maintaining Ca²⁺ homeostasis in the endoplasmic reticulum¹⁴. TTYH1 is a potent driver of tumor microtubule-mediated brain colonization by glioma cells¹⁵ and also functioning as potential biomarkers for triple-negative breast cancer using integrating genomics analysis¹⁶. TTYH2 is the second member of the TTYHs family found to be overexpressed in several cancers like osteosarcoma¹⁷ colon carcinoma¹⁸ and renal cell carcinoma¹⁹. As for the third member of tweety family, TTYH3, whose structure possesses a Ca²⁺-dependent switch from intra to intermembrane dimerization²⁰ encodes a maxi-Cl⁻ channel in the excitable membrane¹³. W et al. found that upregulation of TTYH3 promoted epithelial to mesenchymal transition through Wnt/ β -catenin signaling pathway and inhibited apoptosis in cholangiocarcinoma²¹. However, research on TTYH3 is rarely on the whole and little is known about the association between TTYHs and infiltrating immune cells in any cancer. Therefore, this is the first data mining study to predict the possible role of TTYH3 especially its relationship with immune cell and immunotherapy response in lung cancer.

In this study, we evaluated the expression of TTYH3 and its diagnostic and prognostic value in lung cancer. Additionally, the effects of TTYH3 on the cell proliferation, migration and invasion were determined in lung cancer cells. To further clarify the underlying mechanism of TTYH3 in lung cancer, we constructed the network of TTYH3 and its co-expressed genes and explored the signaling pathways they might be involved in. Based on the enrichment results, the correlation between TTYH3's expression and immune scores, immune infiltration cells and immunotherapy response were further explored, which was proposed to provide a potential target for precision therapy of lung cancer.

Materials And Methods

The expression of TTYH3 in lung cancer compared to normal lung tissue

Three microarray datasets including GSE30219, GSE19188 and GSE31210 were obtained from the Gene Expression Omnibus (GEO) database (<https://www.ncbi.nlm.nih.gov/geo/>)¹³ to analyze the expression of TTYH3 in lung cancer, including different histological subtypes, compared with normal lung tissue. Especially for lung adenocarcinoma (LUAD) and lung squamous cell cancer (LUSC), we used the UALCAN (<http://ualcan.path.uab.edu/index.html>)²² web tool with default settings to explore them from TCGA database. In addition, the tumor tissues and adjacent normal tissues were obtained from 24 patients who were newly

diagnosed with lung cancer. This study has been approved by the Ethics Committee of Medical School of Wuhan University (Wuhan, China).

The identification of TTYH3's diagnosis and prognosis value in lung cancer patient

Receiver operating characteristic (ROC) curves was applied to detect the diagnostic value of TTYH3 in lung cancer, which were derived from GSE19188, GSE30219, GSE31210 and clinical samples, respectively. Furthermore, we analyzed the different expression of TTYH3 between normal and stage 1A patients in both GSE30219 and GSE31210 to better reveal the efficacy of TTYH3 in the early diagnosis of lung cancer. The Kaplan-Meier Plotter (<http://www.kmplot.com>)²³ website was used to identify the prognostic value of TTYH3 in lung cancer. We analyzed overall survival (OS) and post-progression survival (PPS) in all lung cancer samples, LUAD and LUSC. HR with 95% CI and logrank p-values were calculated and extracted from the Kaplan-Meier Plotter, which were shown in the plots.

Cell culture

Lung cancer cell lines A549 and H1299 were cultured in RPMI-1640 medium (Biological Industries, Israel) supplemented with 10% heat-inactivated fetal bovine serum (FBS, Biological Industries, Israel), 1% penicillin/streptomycin (Beyotime Biotechnology, China). In addition, the HEK293T cells, which were used for transfection were cultured in DMEM (Biological Industries, Israel) with 10% FBS and 1% penicillin/streptomycin. The growth of the cells were maintained under humidified conditions at 37°C with 5% CO₂ and their logarithmic growth phases were used for subsequent experiments.

Quantitative real-time PCR (RT-qPCR)

Total RNA was extracted from the clinical samples and cell lines using TRIzol (Invitrogen, Carlsbad, CA, USA) according to the manufacturer's guidance. The RevertAid RT Reverse Transcription Kit (Thermo Fisher Scientific) was used to reverse-transcribe the total RNA (2.0 µg) to cDNA. PCR amplification was performed with the ChamQ SYBR qPCR Master Mix (Q311-02, Vazyme, Nanjing, China) using the QuantStudio 6 Flex Real-Time PCR System (Thermo Fisher Scientific, Waltham, MA, USA). A housekeeping gene (GAPDH) was used to normalize the average CT value of target genes. The expression fold-changes were analyzed by the $2^{-\Delta\Delta C_t}$ relative quantitative methods. The RT-qPCR primer sequences are listed in Table S1.

Lentivirus-mediated short hairpin (sh) RNA transfection

The knockdown plasmid of TTYH3 and the empty control vector (pLenti-CMV-GFP-Puro) were obtained from the Public Protein/Plasmid Library (Nanjing, China). In addition, psPAX2 packaging and pCMV-VSVG envelop plasmids were purchased from Zoman. A 21-nucleotide sequence, named as short hairpin (sh) TTYH3: 5'-GCATCGCAGTGGGATTCTACG-3', corresponding to the targeted TTYH3 mRNA was selected and constructed. 5'-GTTCTCCGAACGTGTACGTT-3' was used as the negative control. Lentivirus was produced in HEK293T cells using PEI according to the instruction. For transduction, 3×10^5 target lung cancer cells were incubated with 0.5 ml lentiviral supernatant containing polybrene (8µg/mL) (Santa cruz, Germany) and 1.5ml RPMI-1640. After 48 hours, the cells were selected under the pressure of puromycin. Finally, the efficiency of the knockdown was verified by RT-qPCR and western blotting.

CCK8 assay

Viability of A549 cells was assessed using CCK8 assays (C0038; Dojindo Molecular Technology, Tokyo, Japan) according to the manufacturer's instructions. The absorbance values were measured after transfection to evaluate the effect of TTYH3-knockdown on cell proliferation. Firstly, cells were seeded into 96-well plates at a density of 3×10^3 /well and incubated overnight followed by the addition of 10 μ l CCK8 solution to each well and incubation for another 1 h. Absorbance was measured at 450 nm with a micro-plate reader at 0, 24, 48, 72 and 96 h after CCK8 was added.

Flow cytometry assay

The cells were washed with PBS (2000rpm, 5min) once and the concentration was adjusted to 1×10^6 /ml. After centrifuging the prepared single-cell suspension, 500ul of 70% cold ethanol was added into the cells for 2 hours in order to fix cells. Prior to application, Rnase A: PI was prepared into staining working solution by 1:9 volume. Two hours later, 500 μ L PI/RNase A staining working solution prepared in advance was added into cells, then they were incubated for 30 min at 37°C away from light. The DNA content was detected by flow cytometry. The data were analyzed by Flowjo software. The percentage of cells in the G1 phase, the S phase, and the G2 phase was analyzed.

Transwell migration and invasion assays

Cells were centrifuged at 600 g for 5 min at room temperature after trypsinizing and then washed with RPMI-1640 medium twice in order to eliminate the effect of FBS. For the invasion assay, transwell membranes were coated with Matrigel (BD Biosciences), which was diluted 10 times with RPMI-1640 medium. 1×10^4 /chamber cells were resuspended in 200 μ l RPMI-1640 medium and then seeded into the upper chamber of a 24-well chemotaxis chamber with polycarbonate filters (8- μ m pore) (Corning Incorporated, Glendale, AZ, USA). In the lower chamber, 600 μ l RPMI-1640 supplemented with 10% FBS was added. The ability of migration and invasion was determined by counting the number of cells that had successfully migrated through the membrane (migration) or invaded through the Matrigel matrix (invasion). After 24 hours, cells on the upper side of the chamber were removed while cells on the lower side were fixed with 4% paraformaldehyde for 30 min, stained with crystal violet for 10 min and then photographed under the microscope. The number of crystal violet-stained cells was counted in five fields from each well at $\times 200$ magnification.

Wound healing assay

The cells were inoculated in 6-well culture plates with the density of 3×10^5 /well and incubated overnight. After 48 hours, when the confluence was close to 80%, a monolayer of the cells was scratched with a 10- μ l pipette tip and photographed at 0 h, 12 h and 24 h. The areas of the scratches were compared at different time points.

Gene Ontology (GO) and Kyoto Encyclopedia of Genes and Genomes (KEGG) enrichment analyses of TTYH3

We first used Oncomine database to obtain the co-expression profile of TTYH3 followed by the visualization with Enricher web tool (<https://amp.pharm.mssm.edu/Enrichr>)²⁴ and then confirmed these genes' expression in lung cancer cell lines with TTYH3 knocking down. The biological processes or pathways which TTYH3 and its related genes were involved in were detected via GO and KEGG analyses. GO analyses can be divided into three components: molecular function (MF), biological process (BP) and cellular component (CC).

The correlations between TTYH3 and gene markers of immune infiltration cells in LUAD and LUSC

To assess the reliable results of immune score evaluation, RNA-sequencing expression profiles and corresponding clinical information for LUAD and LUSC were downloaded from the TCGA dataset (<https://portal.gdc.com>)²⁵ and we used R software package, *immueconv*, to carry out analysis. The results were visualized by R foundation for statistical computing (2020) version 4.0.3 and software packages *ggplot2* and *heatmap*.

Tumor immune estimation resource (TIMER) is a web tool that can be employed to analyze the tumor-infiltrating immune cells (<https://cistrome.shinyapps.io/timer/>)²⁶. Levels of six tumor-infiltrating immune subsets (B cells, CD4⁺ T cells, CD8⁺ T cells, macrophages, neutrophils, and dendritic cells) are pre-calculated for 10,897 tumors from 32 cancer types. Particularly, the module “correlation” allows the researchers to explore gene-gene associations that may be related to cancer immunity and plot the expression scatterplots between user-defined genes in a given cancer type, together with the Spearman’s correlation and estimated statistical significance. Therefore, we applied this tool to detect TTYH3’s relationship with gene markers of immune infiltrating cells in LUAD and LUSC.

Tumor Immune Dysfunction and Exclusion (TIDE) evaluation of TTYH3 in immune therapy

TIDE (<http://tide.dfci.harvard.edu/>)²⁷ was utilized to estimate the immunotherapy response prediction on TTYH3 of lung cancer. The module “biomarker evaluation” can be used to evaluate the accuracy of TTYH3 as a biomarker on immune checkpoint blockades (ICB) therapy response of lung cancer, which was achieved by comparing correlations with other published ICB biomarkers including CD274 (PD-L1), MSI Score (microsatellite instability score), CD8, Merck18 and IFNG (Interferon-gamma), the performance was represented by the area under the curve (AUC).

Furthermore, potential ICB response was predicted with TIDE algorithm by virtue of RNA-sequencing expression profiles and corresponding clinical information for lung cancer. TIDE algorithm uses a set of gene expression markers to evaluate tumor immune escape mechanisms, and higher TIDE score means poorer efficacy of ICB therapy and shorter survival after ICB treatment.

Statistical analysis

The expression of TTYH3 in different groups was compared using 2-tailed t-test and one-way ANOVA followed by Dunnett's test. The association between TTYH3 expression and clinic-pathological features was detected via the χ^2 test. A Cox proportional hazards regression model was applied for the univariate and multivariate analyses of survival. *p* value < 0.05 was considered statistically significant.

Results

TTYH3 is upregulated in lung cancer in both databases and clinical samples

In order to examine the expression of TTYH3 in lung cancer, we assessed the published data for cancer and normal tissues from the GEO and TCGA databases. The results showed a significant up-regulation of TTYH3 in lung cancer compared to normal tissue ($p < 0.0001$) in GSE31210 (Fig. 1A). GSE19188 showed that in different histological subtypes, including ADC ($p < 0.0001$), SCC ($p < 0.0001$) and LCC ($p < 0.0001$), TTYH3 had increased expression (Fig. 1B). Furthermore, TTYH3 was also found uniformly upregulated in ADC ($p < 0.0001$), BAS ($p < 0.0001$), LCC ($p < 0.01$), LCNE ($p < 0.0001$), SCC ($p < 0.001$), SQC ($p < 0.0001$) of GSE30219 (Fig. 1C). Consistently, comparison of TTYH3 gene expression in the RNA-seq data from TCGA demonstrated the upregulation of TTYH3 in both LAUD and LUSC (Fig. 1D, E). Biopsy specimens obtained from 24 lung cancer patients enrolled in this study further showed a significant up-regulation of TTYH3 in lung cancer tissues compared to non-tumor tissue ($p < 0.05$) (Fig. 1F,G).

TTYH3 has a high diagnostic value in lung cancer

The GEO datasets were employed to explore the diagnostic potential of TTYH3 in lung cancer. TTYH3 showed a high diagnostic accuracy in GSE19188 with AUC=0.829 (95% CI 0.764-0.894, $p < 0.0001$) (Fig. 2A), in GSE30219 with AUC=0.851 (95% CI 0.759-0.942, $p < 0.0001$) (Fig. 2B) and in GSE31210 with AUC=0.832 (95% CI 0.732-0.917, $p < 0.0001$) (Fig. 2C). Additionally, analysis of the patient cohort revealed the AUC=0.733 (95% CI 0.592-0.873) (Fig. 2D). Finally, the TTYH3 expression in patients with their early stage (stage 1A) were analyzed and found that AUC value was 0.850 (95% CI 0.757-0.943) (Fig. 2E, F) in GSE30219 and 0.775 (95% CI 0.678-871) (Fig. 2G, H) in GSE31210. These results revealed that TTYH3 had a high diagnostic performance in differentiating lung cancer patients from normal individuals, even for the early stages of lung cancer. In addition, we further analyzed the association between TTYH3 expression and clinico-pathological characteristics of patients. A chi-square test found the relationship between the expression of TTYH3 and gender ($p = 0.0234$), smoke ($p = 0.0115$), final stage ($p = 0.0023$) and relapse ($p < 0.0001$) from GSE31210 (Table 1).

High expression of TTYH3 is a predictor of poor prognosis in lung cancer

We detected the prognostic value of TTYH3 in lung cancer patient by using the Kaplan-Meier Plotter database and GEO datasets. Patients were split into two groups according to the median expression of TTYH3 with high and low, respectively. The Kaplan-Meier Plotter analysis revealed that among all lung cancer patients, high expression of TTYH3 indicated poorer OS than those with low expression (HR=1.48[1.25-1.74], logrank $p = 3.5E-06$) (Fig. 3A), and LUAD patients (HR=2.39[1.85-3.08], logrank $p = 6.7E-12$) (Fig. 3B) as well as LUSC patients (HR=0.81[0.6-1.11], logrank $p = 0.19$) (Fig. 3C). Except for OS, higher TTYH3 expression also predicted a worse PPS for all lung cancer samples (HR=2.09[1.35-3.22], logrank $p = 0.00073$), LUAD patients (HR=1.98[1.21-3.25], logrank $p = 0.0058$) and LUSC patients (HR=0.44[0.14-1.33], logrank $p = 0.14$) (Fig. 3D-F).

TTYH3 promotes the proliferation of lung cancer cells

To gain insights into the biological function of TTYH3 in lung cancer, the lung cancer cell lines including A549 and H1299 were selected for stable transfection with shTTYH3 or control vector, respectively. RT-qPCR was used to evaluate the efficiency of knockdown TTYH3 in A549 and H1299 cells (Fig. 4A, D). No marking difference in the migration and invasion between the vector group and shTTYH3 was observed ($p > 0.05$, Fig. 4G) and wound healing assay also validated that ($p > 0.05$, Fig. 4H). However, knockdown of TTYH3 significantly suppressed the proliferation of A549 cells via CCK8 assay ($p < 0.001$, Fig. 4B), which was confirmed in another lung cancer cell line, H1299 (Fig. 4E). The results from flow cytometry consistently showed that knockdown TTYH3 expression

led to the decreased cell number of S stage which meant that the proliferation ability was impaired in both two cell lines ($p < 0.05$, Fig. 4C, F).

GO and KEGG enrichment analysis of TTYH3 and its co-expression genes

To further investigate the tumor promoting effect of TTYH3, we used Oncomine database to identify the TTYH3 co-expression network and then obtained 20 related genes which were positively correlated with TTYH3 in lung cancer (Fig. 5A, Table 2). Subsequently, the molecules that were most significantly related to the expression of TTYH3 were selected to verify the expression at mRNA level. In A549 cells, after knocking down the expression of TTYH3, the expressions of IQCE, BRAT1, FTSJ2, CARD11, CHST12, AMZ1, SNX8 and NUDT1 were subsequently decreased and the decreases of FTSJ2 ($p < 0.05$), CARD11 ($p < 0.0001$), AMZ1 ($p < 0.01$) and SNX8 ($p < 0.01$) were statistically significant (Fig. 5B). A consistent result was also observed in H1299 cell line (Fig. 5C), the expression of all molecules significantly correlated with TTYH3 decreased after TTYH3 knockdown, and IQCE ($p < 0.01$), BRAT1 ($p < 0.05$), CARD11 ($p < 0.0001$), CHST12 ($p < 0.01$), AMZ1 ($p < 0.001$) and SNX8 ($p < 0.01$) were statistically significant. The validation of the above molecules at mRNA level laid a foundation for subsequent analysis.

Therefore, GO and KEGG were employed to analyze the potential role of TTYH3 and its co-expression genes. The results showed a strong correlation with immune-related signaling pathways. The ten pathways in which these genes were enriched included of O-glycan biosynthesis, Notch signaling pathway, Glycosaminoglycan biosynthesis, Long-term depression, B cell receptor signaling pathway, NF-kappa B signaling pathway, T cell receptor signaling pathway, Parathyroid hormone synthesis, secretion and action, Sphingolipid signaling pathway and Vascular smooth muscle contraction (Fig. 6A). In addition, GO analysis of TTYH3 and its related genes was performed, which included 3 different components. The BP was enriched in marginal zone B cell differentiation, TORC1 signaling, mature B cell differentiation involved in immune response, negative regulation of embryonic development and dermatan sulfate biosynthetic process (Fig. 6B). As for MF, the genes were mainly enriched in chondroitin sulfotransferase activity, nucleoside-triphosphate diphosphatase activity, volume-sensitive anion channel activity, filamin binding and guanylate kinase activity (Fig. 6C). TTYH3 and its positively co-expressed genes were primarily associated with T cell receptor complex in CC (Fig. 6D).

The association between TTYH3 expression and immune infiltration in lung cancer

In view of the outcomes that the GO and KEGG analysis of TTYH3 and its correlated genes in lung cancer showing significant relationship with T and B cells in immunity, CIBERSORT algorithm was used to evaluate the immune scores of lung cancer samples with high and low TTYH3 expression. According to the median value of TTYH3 expression, the samples in LUAD were divided into high expression TTYH3 group and low expression TTYH3 group and the infiltration ratio of immune cells in different groups was calculated respectively. As it was seen from Fig.7A, B cell memory ($p < 0.05$), B cell plasma ($p < 0.001$), T cell CD4⁺ memory resting ($p < 0.001$), T cell regulatory (Treg, $p < 0.05$), T cell gamma delta ($p < 0.05$), NK cells resting ($p < 0.01$), NK cell activated ($p < 0.05$), M₀, M₁, M₂ Macrophage ($p < 0.001$) and Mast cell activated ($p < 0.05$) were statistically different in infiltration ratio between the two groups. Fig.7B shows the differences in immune cell infiltration in LUSC tissues between the high-expression and low-expression TTYH3 groups. B cell naive ($p < 0.05$), B cell plasma ($p < 0.001$), T cell CD8⁺ ($p < 0.001$), T cell CD4⁺ memory resting ($p < 0.01$), T cell CD4⁺ memory activated ($p < 0.001$), T cell

gamma delta ($p < 0.001$), NK cell resting ($p < 0.05$), M₀ Macrophage ($P < 0.001$) and M₁ Macrophage ($p < 0.01$) had statistical difference in infiltration ratio between the two groups.

The results of the above immune score confirmed that the difference in TTYH3 expression would lead to the difference in the level of immune cell infiltration in LUAD and LUSC, so we further explored the association between TTYH3 expression and tumor purity and infiltrating levels of immune cells by using TIMER online website. The outcomes displayed that TTYH3 expression showed a slight correlation with tumor purity in LUAD and LUSC. In LUAD, no correlation between TTYH3 expression and the infiltration of B cell was found (Fig. 8B) and CD8⁺ T cell (Fig. 8C) and so was in LUSC. However, the expression of TTYH3 was significantly positively correlated with the infiltration of CD4⁺ T cells ($cor=0.341$, $p=1.29E-14$), macrophage ($cor=0.252$, $p=1.77E-08$), neutrophil ($cor=0.35$, $p=2.27E-15$) and dendritic cell ($cor=0.353$, $p=9.68E-16$) in LUAD (Fig. 8D-F) and the similar outcomes is evident in LUSC (Fig. 8K-N).

To further elucidate the relationship between TTYH3 and immune infiltration, we analyzed correlations between TTYH3 and immune markers of immune cells (Table 3) both in LUAD and LUSC. In LUAD, the expression of TTYH3 was obviously correlated with the major biomarkers of monocyte, tumor-associated macrophage, M₁ macrophage, M₂ macrophage, neutrophil, dendritic cell and different functional T cells (Th1, Th2, Tfh, Th17, Treg), which was consistent with the outcomes obtained from Fig. 8. However, we couldn't see such a conclusive result in LUSC as showed in LUAD, showing a strong correlations with monocyte, tumor-associated macrophage, neutrophil, dendritic cell, Th1, Th2 and Treg cells.

TTYH3 owned a predictive value for immunotherapy response in lung cancer

Recent advances in ICBs therapy like targeting programmed cell death protein 1 (PD-1) / PD-ligand 1 (PD-L1) and cytotoxic T-lymphocyte-associated protein 4 (CTLA-4) has provided clinical benefits for patients with lung cancer, but the majority still do not respond. Although a few biomarkers of ICB treatment response have been developed, the predictive power of these biomarkers showed substantial variation across datasets^{28,29}. To evaluate immunotherapy predictive value of TTYH3, we utilized the TIDE web tool, which is a computational framework developed to evaluate potential of tumor immune escape based on the gene expression profiles of cancer samples. The area under the ROC curve (AUC) were assessed for TTYH3 expression in comparison with existing biomarker signatures, which functioned as a tool for predicting response to immunotherapy. From these five different study cohorts on lung cancer, TTYH3 as a biomarker showed good performance of immunotherapy response with the AUC > 0.5. (Fig. 9A-B, Table 4).

However, TTYH3 is highly expressed in lung cancer tissues. Is the patient's response to immunotherapy high or low? We further explored that using R language based on TIDE algorithm. As shown in Fig.9C, TIDE scores of patients in the high TTYH3 expression group were higher than those in the low expression group, and the results showed a statistically significant difference ($p < 0.0001$). TIDE algorithm uses a set of gene expression markers to assess the immune escape mechanism of tumors, so patients with high TTYH3 expression had a shorter survival after immunotherapy.

Discussion

Lung cancer remains the most commonly diagnosed cancer and the leading cause of cancer death globally¹. Novel approaches including immunotherapy have improved survival in several cases of advanced stage. However, the survival rate of long responders still remains below 20%^{30,31}. In the tumor microenvironment, the invasion of immune cells is considered to be closely related to the poor prognosis of tumors^{3,4}, and the evaluation of the invasion of immune cells in tumors can be used to predict tumor recurrence and death⁶⁻⁸. Therefore, it is of great significance to find a biomarker that can comprehensively reflect tumor cells and the infiltration of immune cells for the diagnosis, treatment and prognosis of lung cancer. Here, we found TTYH3 promoting cell proliferation and related to immune cell infiltration was associated with the prognosis of and immunotherapy response in lung cancer using the transcriptome-seq data and clinical features obtained from TCGA.

In this study, we assessed the expression of TTYH3 in lung cancer using the GEO databases, TCGA database and clinical samples, revealing elevated TTYH3 level in lung cancer. Furthermore, TTYH3 possessed promising diagnostic value in distinguishing lung cancer patients from healthy individuals based on the evidence obtained from the ROC curves results. Meanwhile, Kaplan-Meier plotters revealed that high expression of TTYH3 might be defined as a risk factor that affected the OS and PPS of lung cancer patients. Patients with a high level of TTYH3 were more likely to present with disease in a late TNM stage and tended to relapse. Taken together, these results suggest that TTYH3 may possess diagnostic and prognostic biomarker potentials for lung cancer.

In order to clarify the potential regulatory mechanism of TTYH3 in lung cancer, we first examined the effect of TTYH3 on the proliferation, migration and invasion of lung cancer cells. Knockdown of TTYH3 expression significantly decreased the proliferation of lung cancer cells, and inhibition of cell proliferation was considered to be related to the prognosis of lung cancer patients^{32,33}. Furthermore, we found that IQCE, C7orf27, LFNG, AMZ1, FTSJ2, NUDT1, SNX8, EIF38, CHST12 and so on had a great relationship with TTYH3, GO and KEGG analyses showed that TTYH3 and its co-expressed genes had a strong correlation with immune-related signaling pathways. The pathways in which these genes were enriched included B cell and T cell receptor signaling pathway. GO analysis showed the enrichment of marginal zone B cell differentiation, mature B cell differentiation involved in immune response and T cell receptor complex.

An additional key finding in this study was the correlation of TTYH3 expression with the degree of immune infiltration and response to immunotherapy in lung cancer. The role of the immune system in cancer development and progression is of a paramount importance^{34,35}. In this part of analyses, we firstly divided lung cancer samples into high expression group and low expression group according to the difference in the expression of TTYH3. CIBERSORF algorithm was used to analyze and it was found that there were significant differences in the infiltrating proportion of some immune cells in two groups, including B cell plasma, T cell CD4⁺ memory resting, Treg, T cell gamma delta, NK cell resting, M₀ and M₁ Macrophage. Subsequently, by using of TIMER website we found that TTYH3 expression was significantly positively correlated with infiltration of monocytes, TAM, M₁ macrophages, M₂ macrophages, Th1, Tfh and Treg as well as T cell exhaustion, indicating that the high expression of TTYH3 was correlated with the level of TAMs, Treg, CD4⁺ T cell infiltration and T cell exhaustion in lung cancer.

In lung cancer microenvironment, there are a set of immune infiltration cells including dendritic cells, TAMs, T cells and natural killer cells³⁶, which play an important regulatory role in tumor progression and are often

accompanied by poor prognosis of patients³⁷. TAMs is highly heterogeneous and has diversity or even opposite biological characteristics, such as M₁ macrophages (classically activated macrophages) and M₂ macrophages (alternately activated macrophages). The M₁/M₂ ratio determines the occurrence and development of tumors, immune escape and subsequent drug resistance processes³⁸. In addition, it has been reported that infiltration of M₀ macrophages predicts worse OS in LUAD patients³⁹. Xiang et al. have confirmed that PCOLCE could become a potent prognostic biomarker due to its association with the infiltrating TAM in gastric cancer⁴⁰. Accumulating evidence suggests that the recruitment of Treg helps cancer cells to immune escape through various mechanisms⁴¹, and Treg accumulation could predict worse prognosis in several tumors of epithelial origin⁴²⁻⁴⁴. Biomarkers such as ERBB1/2/3⁴⁵, LAIR2⁴⁶, EEF1E1⁴⁷ and so on closely related to the infiltration level of Treg predicted the outcome of several cancers. T cell exhaustion, a stage of T cells dysfunction, is defined by poor effector function, sustained expression of inhibitory receptors and a transcriptional state distinct from that of functional effector or memory T cells⁴⁸. T cell exhaustion exacerbates optimal control of infection and tumors, which may lead to poor prognosis in patients⁴⁹. Further analysis showed that TTYH3 was associated with most infiltrating immune cells in LUAD, but only with a few cells in LUSC, which partly explains why the prognostic value of TTYH3 in LUAD was higher than that in LUSC.

Immunotherapy has revolutionized the treatment of cancer. Modern cancer immune therapy developed over more than 50 years, which was first applied in hematological malignancies^{50,51}. As for solid tumors, many years of basic and clinical research provided the rationale to investigate ICB and treatment modalities ranged from cell therapy using tumor-specific T cells, including those that express transgenic T cell receptors (TCRs) and chimeric antigen receptors (CARs), to antibodies targeting important immunological checkpoint molecules, such as PD1⁵². Unfortunately, many patients fail to respond to immunotherapy. Therefore, the identification of novel methods to enhance the efficacy of immunotherapeutic modalities is an area of active investigation. By virtue of biomarker evaluation module from TIDE website, the accuracy of TTYH3 on five ICB lung cancer cohorts in comparison with other published biomarkers associated with tumor immune evasion including CD274 (PD-L1), MSI Score, CD8, Merck18 and IFNG were evaluated and we found that TTYH3 could predict a strong likelihood of response to immunotherapy. Further R analysis showed that patients with high TTYH3 expression had poor response to ICB treatment and shorter survival after immunotherapy, which was consistent with our conclusion that patients with high TTYH3 expression had worse prognosis.

However, there are some notable limitations. First, the result that TTYH3 possessed a potential diagnosis and prognosis value was only obtained from online public databases and 24 patients' samples, which needed to collect a large number of clinical samples to validate. Similarly, the correlation between TTYH3 and immune infiltration and immune therapy response was also accomplished from website and R analysis, we have to carry out *in vivo* experiments to confirm that. Second, the GO and KEGG enrichment results showed that TTYH3 and its co-expressed genes took apart in the immune related pathways, however we just deeply explored the association of TTYH3 and immune infiltration cells. How does TTYH3 and its co-expressed genes participate in the mechanism regulatory of immune pathway, and as a kind of chloride ion channel, Does TTYH3 itself exert any special function in regulating immune pathway? These all need to be further studied in the future.

Conclusion

In conclusion, we found that TTYH3 is upregulated in lung cancer, and it may act as an early stage diagnostic marker in lung cancer patients. High expression of TTYH3 is associated with poor prognosis in lung cancer both LUAD and LUSC. Moreover, TTYH3 promotes the proliferation of lung cancer cell, is positively associated with immune infiltration and might be a biomarker representing immunotherapy response. This study might provide significant clinical implications for guiding tailored anti-TTYH3 therapy in combination with immunotherapy and a potential target for the diagnosis and treatment of lung cancer. However, a large number of clinical samples and animal experiments are needed to verify the above conclusions.

Abbreviations

TTYH3

Tweety family member 3

GEO

Gene Expression Omnibus

TCGA

The Cancer Genome Atlas

ROC

Receiver operating characteristic

GO

Gene ontology

KEGG

Kyoto Encyclopedia of Genes and Genomes

MF

Molecular function

BP

biological process

CC

cellular component

TIMER

Tumor immune estimation resource

TIDE, tumor immune dysfunction and exclusion

LUAD

Lung adenocarcinoma

LUSC

Lung squamous cell cancer

ADC

adenocarcinoma

BAS

basaloid

LCC

large cell carcinoma

LCNE

large cell neuroendocrine tumor

SCC
small cell carcinoma
SQC
squamous cell carcinoma
OS
Overall survival
PPS
Post-progression survival
HR
hazard ratio
CI
confidence interval
ICB, immune checkpoint blockade.

Declarations

Acknowledgements

We acknowledge and appreciate our colleagues for their valuable efforts and comments on this paper.

Authors' contributions

ZQP designed the whole study, WZM and ZXR performed the experiments, analyzed the data and wrote the main manuscript text, LYF, HHJ, Jamal and ZCJ revised the manuscript, THY and XSP provided professional advice about the research. All authors have read and approved the final manuscript.

Funding

This work was supported by the National Natural Science Foundation of China (Nos. 81770180) and Hubei Provincial Natural Science Fund for Creative Research Groups (2018CFA018).

Disclosure

The authors declare that they have no competing interests or personal relationships that could have appeared to influence the work reported in this paper.

References

1. Bray, F. *et al.* Global cancer statistics 2018: GLOBOCAN estimates of incidence and mortality worldwide for 36 cancers in 185 countries. *CA Cancer J Clin* **68**, 394-424, doi:10.3322/caac.21492 (2018).
2. Hirsch, F. R. *et al.* Lung cancer: current therapies and new targeted treatments. *Lancet* **389**, 299-311, doi:10.1016/S0140-6736(16)30958-8 (2017).
3. Wojas-Krawczyk, K. & Kubiowski, T. Imperfect Predictors for Lung Cancer Immunotherapy-A Field for Further Research. *Front Oncol* **10**, 568174, doi:10.3389/fonc.2020.568174 (2020).

4. Chen, D. S. & Mellman, I. Elements of cancer immunity and the cancer-immune set point. *Nature* **541**, 321-330, doi:10.1038/nature21349 (2017).
5. Nguyen, T. T. *et al.* A lepidic gene signature predicts patient prognosis and sensitivity to immunotherapy in lung adenocarcinoma. *Genome Med* **14**, 5, doi:10.1186/s13073-021-01010-w (2022).
6. Galon, J. *et al.* Type, density, and location of immune cells within human colorectal tumors predict clinical outcome. *Science* **313**, 1960-1964, doi:10.1126/science.1129139 (2006).
7. Pages, F. *et al.* International validation of the consensus Immunoscore for the classification of colon cancer: a prognostic and accuracy study. *Lancet* **391**, 2128-2139, doi:10.1016/S0140-6736(18)30789-X (2018).
8. Wang, Y. *et al.* The Immunoscore system predicts prognosis after liver metastasectomy in colorectal cancer liver metastases. *Cancer Immunol Immunother* **67**, 435-444, doi:10.1007/s00262-017-2094-8 (2018).
9. Grabovska, Y. *et al.* Pediatric pan-central nervous system tumor analysis of immune-cell infiltration identifies correlates of antitumor immunity. *Nat Commun* **11**, 4324, doi:10.1038/s41467-020-18070-y (2020).
10. Chen, R. Q., Liu, F., Qiu, X. Y. & Chen, X. Q. The Prognostic and Therapeutic Value of PD-L1 in Glioma. *Front Pharmacol* **9**, 1503, doi:10.3389/fphar.2018.01503 (2018).
11. Han, Y. E. *et al.* Tweety-homolog (Ttyh) Family Encodes the Pore-forming Subunits of the Swelling-dependent Volume-regulated Anion Channel (VRAC_{swell}) in the Brain. *Exp Neurobiol* **28**, 183-215, doi:10.5607/en.2019.28.2.183 (2019).
12. Okada, Y. Tweety Homologs (TTYH) Freshly Join the Journey of Molecular Identification of the VRAC/VSOR Channel Pore. *Exp Neurobiol* **28**, 131-133, doi:10.5607/en.2019.28.2.131 (2019).
13. Suzuki, M. & Mizuno, A. A novel human Cl⁻ channel family related to Drosophila flightless locus. *J Biol Chem* **279**, 22461-22468, doi:10.1074/jbc.M313813200 (2004).
14. Kumada, T. *et al.* Ttyh1, a Ca²⁺-binding protein localized to the endoplasmic reticulum, is required for early embryonic development. *Dev Dyn* **239**, 2233-2245, doi:10.1002/dvdy.22348 (2010).
15. Jung, E. *et al.* Tweety-Homolog 1 Drives Brain Colonization of Gliomas. *J Neurosci* **37**, 6837-6850, doi:10.1523/JNEUROSCI.3532-16.2017 (2017).
16. Zhong, G., Lou, W., Shen, Q., Yu, K. & Zheng, Y. Identification of key genes as potential biomarkers for triplenegative breast cancer using integrating genomics analysis. *Mol Med Rep* **21**, 557-566, doi:10.3892/mmr.2019.10867 (2020).
17. Moon, D. K., Bae, Y. J., Jeong, G. R., Cho, C. H. & Hwang, S. C. Upregulated TTYH2 expression is critical for the invasion and migration of U2OS human osteosarcoma cell lines. *Biochem Biophys Res Commun* **516**, 521-525, doi:10.1016/j.bbrc.2019.06.047 (2019).
18. Toiyama, Y. *et al.* TTYH2, a human homologue of the Drosophila melanogaster gene tweety, is up-regulated in colon carcinoma and involved in cell proliferation and cell aggregation. *World J Gastroenterol* **13**, 2717-2721, doi:10.3748/wjg.v13.i19.2717 (2007).
19. Rae, F. K. *et al.* TTYH2, a human homologue of the Drosophila melanogaster gene tweety, is located on 17q24 and upregulated in renal cell carcinoma. *Genomics* **77**, 200-207, doi:10.1006/geno.2001.6629 (2001).
20. Li, B., Hoel, C. M. & Brohawn, S. G. Structures of tweety homolog proteins TTYH2 and TTYH3 reveal a Ca²⁺-dependent switch from intra- to intermembrane dimerization. *Nat Commun* **12**, 6913, doi:10.1038/s41467-021-27283-8 (2021).

21. Xue, W. *et al.* Upregulation of TTYH3 promotes epithelial-to-mesenchymal transition through Wnt/beta-catenin signaling and inhibits apoptosis in cholangiocarcinoma. *Cell Oncol (Dordr)* **44**, 1351-1361, doi:10.1007/s13402-021-00642-9 (2021).
22. Chandrashekar, D. S. *et al.* UALCAN: A Portal for Facilitating Tumor Subgroup Gene Expression and Survival Analyses. *Neoplasia* **19**, 649-658, doi:10.1016/j.neo.2017.05.002 (2017).
23. Szasz, A. M. *et al.* Cross-validation of survival associated biomarkers in gastric cancer using transcriptomic data of 1,065 patients. *Oncotarget* **7**, 49322-49333, doi:10.18632/oncotarget.10337 (2016).
24. Kuleshov, M. V. *et al.* Enrichr: a comprehensive gene set enrichment analysis web server 2016 update. *Nucleic Acids Res* **44**, W90-97, doi:10.1093/nar/gkw377 (2016).
25. Tomczak, K., Czerwinska, P. & Wiznerowicz, M. The Cancer Genome Atlas (TCGA): an immeasurable source of knowledge. *Contemp Oncol (Pozn)* **19**, A68-77, doi:10.5114/wo.2014.47136 (2015).
26. Li, T. *et al.* TIMER: A Web Server for Comprehensive Analysis of Tumor-Infiltrating Immune Cells. *Cancer Res* **77**, e108-e110, doi:10.1158/0008-5472.CAN-17-0307 (2017).
27. Fu, J. *et al.* Large-scale public data reuse to model immunotherapy response and resistance. *Genome Med* **12**, 21, doi:10.1186/s13073-020-0721-z (2020).
28. Tang, T. *et al.* Advantages of targeting the tumor immune microenvironment over blocking immune checkpoint in cancer immunotherapy. *Signal Transduct Target Ther* **6**, 72, doi:10.1038/s41392-020-00449-4 (2021).
29. Jiang, Z., Zhou, Y. & Huang, J. A Combination of Biomarkers Predict Response to Immune Checkpoint Blockade Therapy in Non-Small Cell Lung Cancer. *Front Immunol* **12**, 813331, doi:10.3389/fimmu.2021.813331 (2021).
30. Topalian, S. L., Taube, J. M., Anders, R. A. & Pardoll, D. M. Mechanism-driven biomarkers to guide immune checkpoint blockade in cancer therapy. *Nat Rev Cancer* **16**, 275-287, doi:10.1038/nrc.2016.36 (2016).
31. Hellmann, M. D. *et al.* Nivolumab plus Ipilimumab in Lung Cancer with a High Tumor Mutational Burden. *N Engl J Med* **378**, 2093-2104, doi:10.1056/NEJMoa1801946 (2018).
32. Sun, X. *et al.* Overexpression of long non-coding RNA KCNQ10T1 is related to good prognosis via inhibiting cell proliferation in non-small cell lung cancer. *Thorac Cancer* **9**, 523-531, doi:10.1111/1759-7714.12599 (2018).
33. Zhong, M., Wang, W. L. & Yu, D. J. Long non-coding RNA OR3A4 is associated with poor prognosis of human non-small cell lung cancer and regulates cell proliferation via up-regulating SOX4. *Eur Rev Med Pharmacol Sci* **25**, 1762, doi:10.26355/eurrev_202102_25047 (2021).
34. Pardoll, D. M. The blockade of immune checkpoints in cancer immunotherapy. *Nat Rev Cancer* **12**, 252-264, doi:10.1038/nrc3239 (2012).
35. Li, Y. *et al.* A Mini-Review for Cancer Immunotherapy: Molecular Understanding of PD-1/PD-L1 Pathway & Translational Blockade of Immune Checkpoints. *Int J Mol Sci* **17**, doi:10.3390/ijms17071151 (2016).
36. Lavin, Y. *et al.* Innate Immune Landscape in Early Lung Adenocarcinoma by Paired Single-Cell Analyses. *Cell* **169**, 750-765 e717, doi:10.1016/j.cell.2017.04.014 (2017).
37. Noy, R. & Pollard, J. W. Tumor-associated macrophages: from mechanisms to therapy. *Immunity* **41**, 49-61, doi:10.1016/j.immuni.2014.06.010 (2014).

38. Mantovani, A., Bottazzi, B., Colotta, F., Sozzani, S. & Ruco, L. The origin and function of tumor-associated macrophages. *Immunol Today* **13**, 265-270, doi:10.1016/0167-5699(92)90008-U (1992).
39. Zheng, Y. *et al.* A Novel Immune-Related Prognostic Model for Response to Immunotherapy and Survival in Patients With Lung Adenocarcinoma. *Front Cell Dev Biol* **9**, 651406, doi:10.3389/fcell.2021.651406 (2021).
40. Xiang, A. *et al.* PCOLCE Is Potent Prognostic Biomarker and Associates With Immune Infiltration in Gastric Cancer. *Front Mol Biosci* **7**, 544895, doi:10.3389/fmolb.2020.544895 (2020).
41. O'Callaghan, D. S., O'Donnell, D., O'Connell, F. & O'Byrne, K. J. The role of inflammation in the pathogenesis of non-small cell lung cancer. *J Thorac Oncol* **5**, 2024-2036, doi:10.1097/jto.0b013e3181f387e4 (2010).
42. Liyanage, U. K. *et al.* Prevalence of regulatory T cells is increased in peripheral blood and tumor microenvironment of patients with pancreas or breast adenocarcinoma. *J Immunol* **169**, 2756-2761, doi:10.4049/jimmunol.169.5.2756 (2002).
43. Curiel, T. J. *et al.* Specific recruitment of regulatory T cells in ovarian carcinoma fosters immune privilege and predicts reduced survival. *Nat Med* **10**, 942-949, doi:10.1038/nm1093 (2004).
44. Perrone, G. *et al.* Intratumoural FOXP3-positive regulatory T cells are associated with adverse prognosis in radically resected gastric cancer. *Eur J Cancer* **44**, 1875-1882, doi:10.1016/j.ejca.2008.05.017 (2008).
45. Liu, S., Geng, R., Lin, E., Zhao, P. & Chen, Y. ERBB1/2/3 Expression, Prognosis, and Immune Infiltration in Cutaneous Melanoma. *Front Genet* **12**, 602160, doi:10.3389/fgene.2021.602160 (2021).
46. Chen, Z. *et al.* PNOC Expressed by B Cells in Cholangiocarcinoma Was Survival Related and LAIR2 Could Be a T Cell Exhaustion Biomarker in Tumor Microenvironment: Characterization of Immune Microenvironment Combining Single-Cell and Bulk Sequencing Technology. *Front Immunol* **12**, 647209, doi:10.3389/fimmu.2021.647209 (2021).
47. Han, R. *et al.* A Novel HCC Prognosis Predictor EEF1E1 Is Related to Immune Infiltration and May Be Involved in EEF1E1/ATM/p53 Signaling. *Front Oncol* **11**, 700972, doi:10.3389/fonc.2021.700972 (2021).
48. Blank, C. U. *et al.* Defining 'T cell exhaustion'. *Nat Rev Immunol* **19**, 665-674, doi:10.1038/s41577-019-0221-9 (2019).
49. Thommen, D. S. & Schumacher, T. N. T Cell Dysfunction in Cancer. *Cancer Cell* **33**, 547-562, doi:10.1016/j.ccell.2018.03.012 (2018).
50. Rocken, M. Early tumor dissemination, but late metastasis: insights into tumor dormancy. *J Clin Invest* **120**, 1800-1803, doi:10.1172/JCI43424 (2010).
51. Kolb, H. J. *et al.* Donor leukocyte transfusions for treatment of recurrent chronic myelogenous leukemia in marrow transplant patients. *Blood* **76**, 2462-2465 (1990).
52. Waldman, A. D., Fritz, J. M. & Lenardo, M. J. A guide to cancer immunotherapy: from T cell basic science to clinical practice. *Nat Rev Immunol* **20**, 651-668, doi:10.1038/s41577-020-0306-5 (2020)

Tables

Table 1 Correlation of TTYH3 expression and clinicopathological characteristics of patients with lung cancer in GSE31210

Characteristics	No. of patients	TTYH3 expression		chi-square value	p value
		high	low		
Age				2.269	0.1320
≤55	60	25	35		
>55	166	88	78		
Gender				5.141	0.0234
Male	105	61	44		
Female	121	52	69		
Smoke				6.391	0.0115
Ever-smoker	111	65	46		
Never-smoker	115	48	67		
Final Stage				9.278	0.0023
IA-IB	168	74	94		
II	58	39	19		
Repace				19.62	< 0.0001
No	162	66	96		
Yes	64	47	17		

Abbreviation: TTYH3: tweety family member 3

Table 2 TTYH3 and its co-expressed genes in lung cancer from Oncomine database

Gene symbols	Full name	R-Value	P-Value
IQCE	IQ domain-containing protein E	1.000	<0.0001
BRAT1/c7orf27	BRCA1-associated ATM activator 1	1.000	<0.0001
LFNG	Beta-1,3-N-acetylglucosaminyltransferase lunatic fringe	1.000	<0.0001
AMZ1	Archaemetzincin-1	1.000	<0.0001
FTSJ2/MRM2	rRNA methyltransferase 2, mitochondrial	1.000	<0.0001
NUDT1	7,8-dihydro-8-oxoguanine triphosphatase	1.000	<0.0001
SNX8	Sorting nexin-8	1.000	<0.0001
EIF38	Eukaryotic translation initiation factor 3 subunit 8	1.000	<0.0001
CHST12	Carbohydrate sulfotransferase 12	0.936	<0.0001
CARD11	Caspase recruitment domain-containing protein 11	0.936	<0.0001
GNA12	Guanine nucleotide-binding protein subunit alpha-12	0.936	<0.0001
ELFN1	Extracellular leucine-rich repeat and fibronectin type-III domain-containing protein 1	0.936	<0.0001
PSMG3	Proteasome assembly chaperone 3	0.936	<0.0001
TMEM184A	Transmembrane protein 184A	0.936	<0.0001
MAFK	Transcription factor MafK	0.936	<0.0001
INTS1	Integrator complex subunit 1	0.936	<0.0001
MICALL2	MICAL-like protein 2	0.936	<0.0001
UNCX	Homeobox protein unc-4 homolog	0.936	<0.0001
ZFAND2A	Zinc finger, AN-1 type domain 2A	0.936	<0.0001
GPER1	G-protein coupled estrogen receptor 1	0.936	<0.0001

Table 3 Correlation analysis between TTYH3 and relate genes and markers of immune cells in TIMER

Description	Gene markers	LUAD				LUSC			
		None		Purity		None		Purity	
		Cor	P	Cor	P	Cor	P	Cor	P
CD8+ T cell	CD8A	0.092	0.036	0.054	0.227	-0.021	0.686	-0.082	0.072
	CD8B	0.087	0.048	0.053	0.236	0.025	0.576	-0.008	0.861
	CD45(PTPRC)	0.224	***	0.204	***	0.147	**	0.067	0.146
T cell (general)	CD3D	0.074	0.095	0.023	0.607	0.001	0.976	-0.083	0.070
	CD3E	0.117	*	0.074	0.10	0.087	0.051	0.008	0.867
	CD2	0.1	0.023	0.057	0.209	0.031	0.482	-0.051	0.264
B cell	CD19	0.054	0.223	0.001	0.981	0.05	0.262	-0.038	0.402
	CD79A	0.068	0.123	0.027	0.546	0.076	0.091	-0.014	0.763
	CD27	0.088	0.047	0.047	0.295	0.073	0.102	-0.016	0.731
	CD20(KRT20)	-0.014	0.753	0.083	0.064	-0.179	***	-0.169	**
Monocyte	CD14	0.436	***	0.456	***	0.279	***	0.217	***
	CD115 (CSF1R)	0.417	***	0.427	***	0.309	***	0.251	***
TAM	CCL2	0.341	***	0.337	***	0.192	***	0.145	*
	CD68	0.296	***	0.291	***	0.186	***	0.116	0.011
	IL10	0.197	***	0.174	**	0.194	***	0.147	*
M1 Macrophage	INOS (NOS2)	0.197	***	0.177	***	0.002	0.962	0.007	0.877
	CD80	0.251	***	0.23	***	0.14	*	0.071	0.121
	IRF5	0.382	***	0.369	***	0.064	0.156	0.061	0.183
	IL6	0.201	***	0.192	***	0.008	0.852	-0.006	0.890
	CD64(FCGR1A)	0.315	***	0.315	***	0.075	0.095	0	0.996
M2 Macrophage	CD163	0.361	***	0.364	***	0.219	***	0.155	**
	CD206(MRC1)	0.167	**	0.155	**	0.271	***	0.215	***
	VSIG4	0.221	***	0.216	***	0.091	0.041	0.018	0.700
	MS4A4A	0.232	***	0.222	***	0.086	0.056	0.002	0.959
Neutrophil	CD66B(CEACAM8)	-0.086	0.052	-0.092	0.041	-0.042	0.344	0.255	***
	CD11B(ITGAM)	0.398	***	0.41	***	0.336	***	0.282	***
	CD15(FUT4)	0.391	***	0.374	***	0.38	***	0.361	***

Natural killer cell	KIR2DL1	0.014	0.758	0.003	0.955	-0.008	0.856	-0.033	0.473
	KIR2DL3	0.084	0.058	0.068	0.133	-0.003	0.952	-0.034	0.463
	KIR3DL1	0.064	0.141	0.041	0.364	0.103	0.021	0.06	0.191
	KIR3DL2	0.09	0.041	0.073	0.104	-0.046	0.308	-0.086	0.061
	CD56(NCAM1)	0.143	*	0.124	*	0.082	0.067	0.095	0.037
	CD335(NCR1)	0.118	*	0.089	0.049	0.146	*	0.122	*
Dendritic cell	BDCA-1(CD1C)	-0.007	0.875	-0.039	0.383	0.149	**	0.064	0.162
	BDCA-4(NRP1)	0.243	***	0.238	***	0.374	***	0.333	***
	BDCA-3(CD141)	0.09	0.041	0.075	0.097	0.041	0.362	0.023	0.609
	CD123(IL3RA)	0.292	***	0.288	***	0.31	***	0.257	***
Th1	T-bet (TBX21)	0.141	*	0.108	0.016	0.146	*	0.088	0.055
	STAT4	0.173	***	0.126	*	0.241	***	0.189	***
	STAT1	0.291	***	0.273	***	0.071	0.114	0.035	0.446
Th2	GATA3	0.308	***	0.301	***	0.418	***	0.398	***
	STAT6	-0.018	0.686	-0.013	0.780	0.17	**	0.165	**
	IL13	-0.016	0.712	-0.024	0.599	0.016	0.718	-0.028	0.548
Tfh	BCL6	0.169	**	-0.158	**	0.101	0.024	0.114	0.013
	IL21	0.14	*	0.134	*	0.052	0.247	0.013	0.782
Th17	STAT3	0.156	**	0.152	**	0.384	***	0.366	***
	IL17A	-0.001	0.975	-0.034	0.449	-0.012	0.023	-0.139	*
Treg	FOXP3	0.35	***	0.353	***	0.269	***	0.21	***
	CD25(IL2RA)	0.324	***	0.314	***	0.136	*	0.068	0.137
	CCR8	0.284	***	0.271	***	0.216	***	0.151	**
	STAT5B	0.22	***	0.206	***	0.226	***	0.227	***
T cell exhaustion	PD-1 (PDCD1)	0.271	***	0.256	***	0.155	**	0.097	0.034
	CTLA4	0.196	***	0.172	**	0.136	*	0.062	0.179
	LAG3	0.216	***	0.198	***	0.075	0.096	0.023	**
	TIM-3 (HAVCR2)	0.33	***	0.332	***	0.091	0.041	0.01	0.823
	GZMB	0.194	***	0.171	**	0	0.992	-0.067	0.145

Abbreviations: LUAD, lung adenocarcinoma; LUSC, lung squamous cell carcinoma; None, correlation without adjustment; Purity, correlation adjusted by purity; TAM, tumor-associated macrophage; Th, T helper cell; Tfh, Follicular helper T cell; Treg, regulatory T cell; Cor, R value of Spearman's correlation. * P < 0.01; ** P < 0.001; *** P < 0.0001.

Table 4 The AUC of TTYH3 for immunotherapy in lung cancer							
Studies	TIDE	CD274	MSI.Score	CD8	Merck18	IFNG	Custom
Uppaluri2020	0.48	0.69	0.63	0.58	0.65	0.65	0.43
Uppaluri2020	0.54	0.70	0.45	0.48	0.47	0.50	0.64
Ruppin2021	0.51	0.70	0.46	0.75	0.70	0.59	0.60
Prat2017	0.76	0.58	0.41	0.56	0.60	0.62	0
Hee2020	0.57	0.45	0.54	0.56	0.56	0.71	0

AUC, the area under the ROC curve

Figures

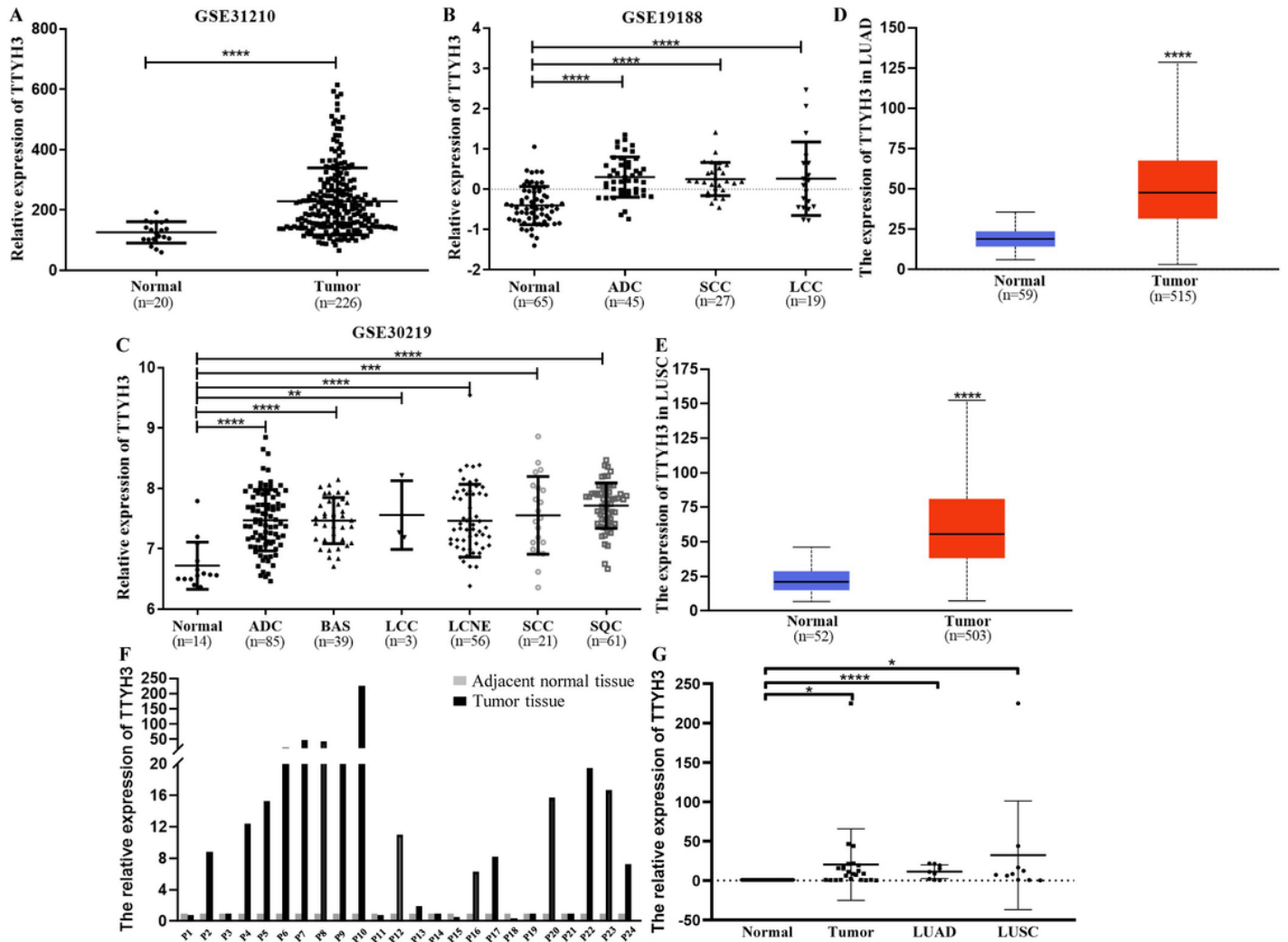


Figure 1

TTYH3 was upregulated in lung cancer tissues. (A) TTYH3's expression in normal tissue and tumor tissue in GSE31210. (B, C) TTYH3's expression in normal tissue and various histological subtypes of lung cancer in GSE19188 and GSE30219. Abbreviation: ADC, adenocarcinoma; BAS, basaloid; LCC, large-cell carcinoma; LCNE, large-cell neuroendocrine tumor; SCC, small cell carcinoma; SQC, Squamous Cell Carcinoma. (D, E) The expression of TTYH3 gene in The Cancer Genome Atlas (TCGA) database: Box plots showing the TTYH3 mRNA expression in LUAD/LUSC tumors and their normal tissues were depicted with red plot and blue plot, respectively. (F, G) TTYH3 mRNA expression from 24 patients' lung cancer tissues and adjacent normal tissues were explored by RT-qPCR. Abbreviation: LUAD, lung adenocarcinoma; LUSC, lung squamous cell carcinoma. **** $p < 0.0001$; *** $p < 0.001$; ** $p < 0.01$.

Figure 2

Diagnostic value of TTYH3 in lung cancer. (A-D) ROC curve for all lung cancer patients in GSE19188, GSE30219, GSE31210 and clinical samples, respectively. (E-H) TTYH3 expression in normal lung and stage 1A lung cancer in

GSE30219 and GSE31210. AUC, area under the receiver operating characteristic curve. **** p < 0.0001.

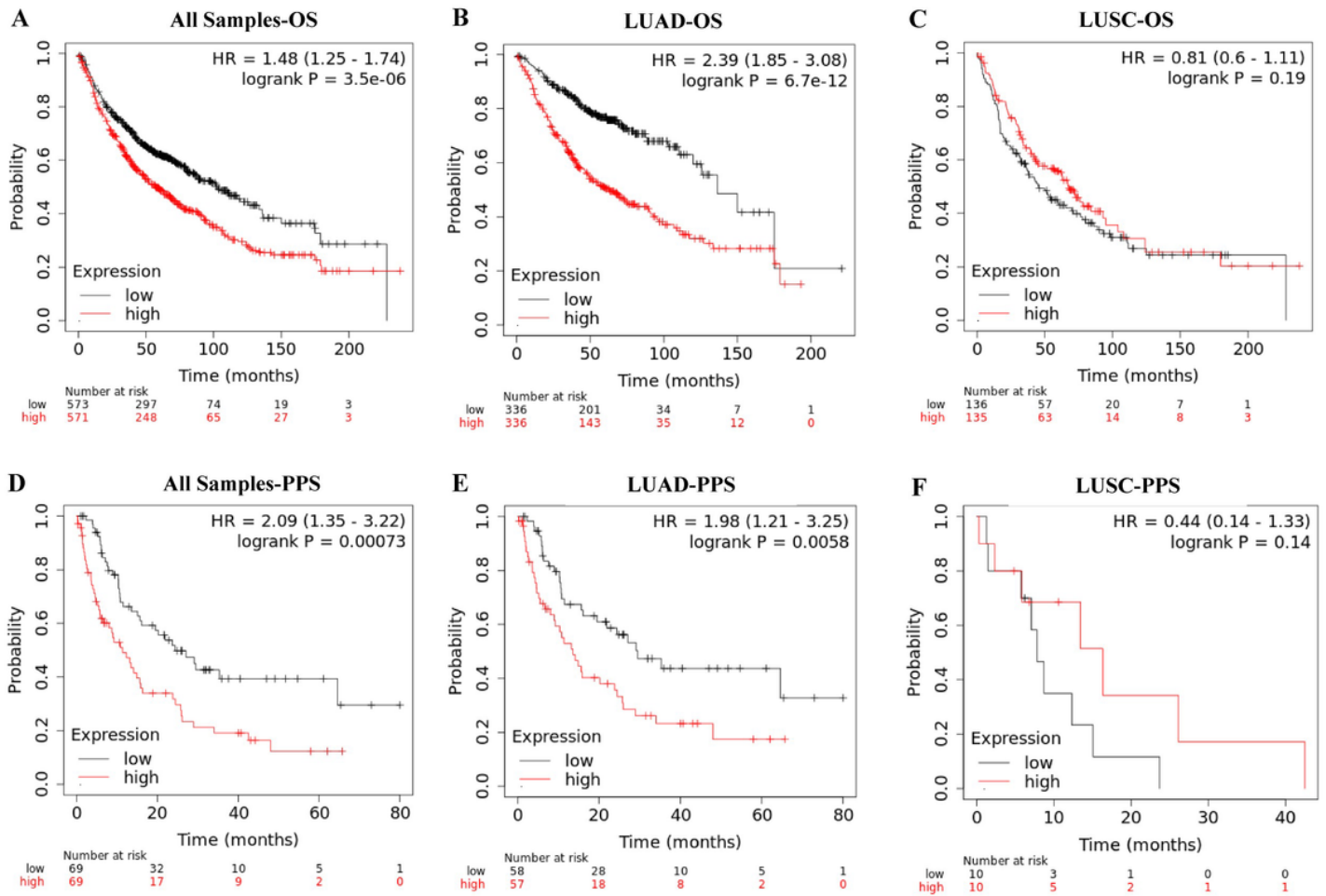


Figure 3

Upregulation of TTYH3 indicated poorer prognosis. The survival curves demonstrated patient survival with high (red) and low (black) TTYH3 expression in lung cancer using Kaplan–Meier plotter tool. (A-C) overall survival (OS); (D-F) post-progression survival (PPS). Abbreviation: LUAD, lung adenocarcinoma; LUSC, lung squamous cell carcinoma. HR, hazard ratio.

Figure 4

Knockdown of TTYH3 reduced the proliferation of lung cancer cells. (A, D) RT-qPCR verified shRNA-mediated inhibition of TTYH3 expression in A549 and H1299 cell lines. (B, E) CCK8 assay detected the changes in proliferation ability of A549 and H1299 cells after sh TTYH3 transfection. (C, F) Flow cytometry assay detected cell cycle change of A549 and H1299 cells after sh TTYH3 transfection. (G) Transwell experiment was performed 24 h after sh TTYH3 transfection. The number of cells on the transwell membrane was compared. The results showed that the ability of migration and invasion was not significant. (H) Wound healing assay showed that the knockdown of TTYH3 didn't affect the migration ability of A549 cells. RT-qPCR, reverse transcription-quantitative

polymerase chain reaction; sh, short hairpin; OD, optical density; ****p < 0.0001; ** p < 0.01; *p < 0.05; ns, not significant.

Image not available with this version

Figure 5

Identification of TTYH3 and its co-expressed genes. (A) The co-expression relationship with TTYH3 was analyzed by Oncomine website; (B, C) RT-qPCR was used to detect the expression of TTYH3 co-expressed molecules at mRNA level in A549 and H1299 cell line, respectively. ns, not significant; * p < 0.05; ** p < 0.01; *** p < 0.001; **** p < 0.0001.

Image not available with this version

Figure 6

Gene ontology (GO) and Kyoto Encyclopedia of Genes and Genomes (KEGG) enrichment analyses of TTYH3 and its co-expression genes. (A) Kyoto Encyclopedia of Genes and Genomes (KEGG) pathways 2019. (B) Enrichment of GO Biological Process (2018) terms in proteomic analysis. (C) Enrichment of GO Molecular Function (2018) terms in proteomic analysis. (D) Enrichment of GO Cellular Component (2018) terms in proteomic analysis. The ratio of the percent composition of terms in proteomic data versus percent composition in the genome annotation was performed in bar graph. The length of the bar means the significance of that specific gene-set or term, and the significance rises as the bar goes deeper.

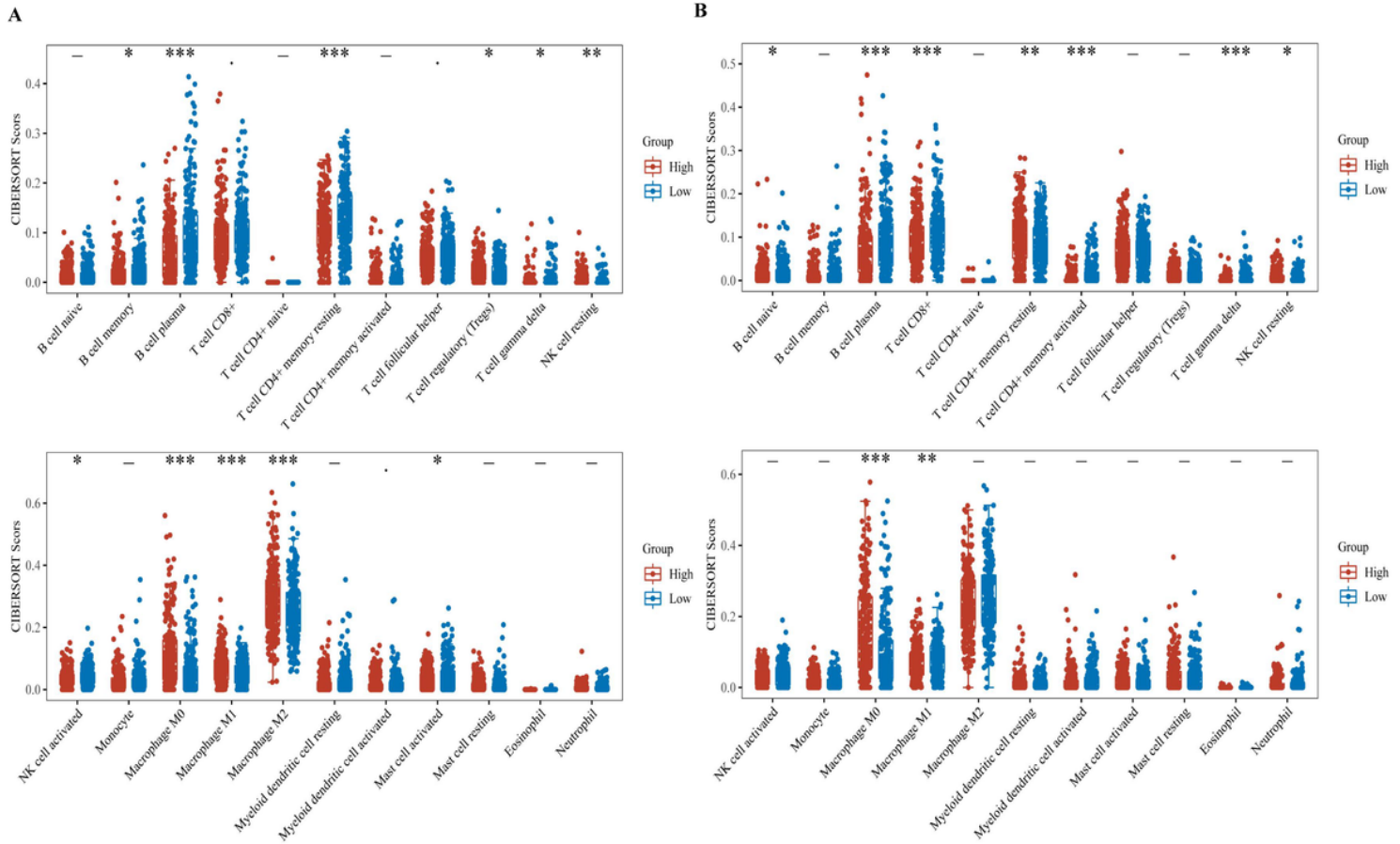


Figure 7

The expression distribution of CIBERSORT immune score in TTYH3 high expression tissues and low expression tissues. (A) The abscissa represents immune cell types, and the ordinate represents the expression distribution of immune score in different groups, which also represents the infiltration ratio of immune cells in LUAD; (B) The same outcomes detected in LUSC. Abbreviation: LUAD, lung adenocarcinoma; LUSC, lung squamous cell carcinoma. ns, not significant; * $p < 0.05$; ** $p < 0.01$; *** $p < 0.001$.

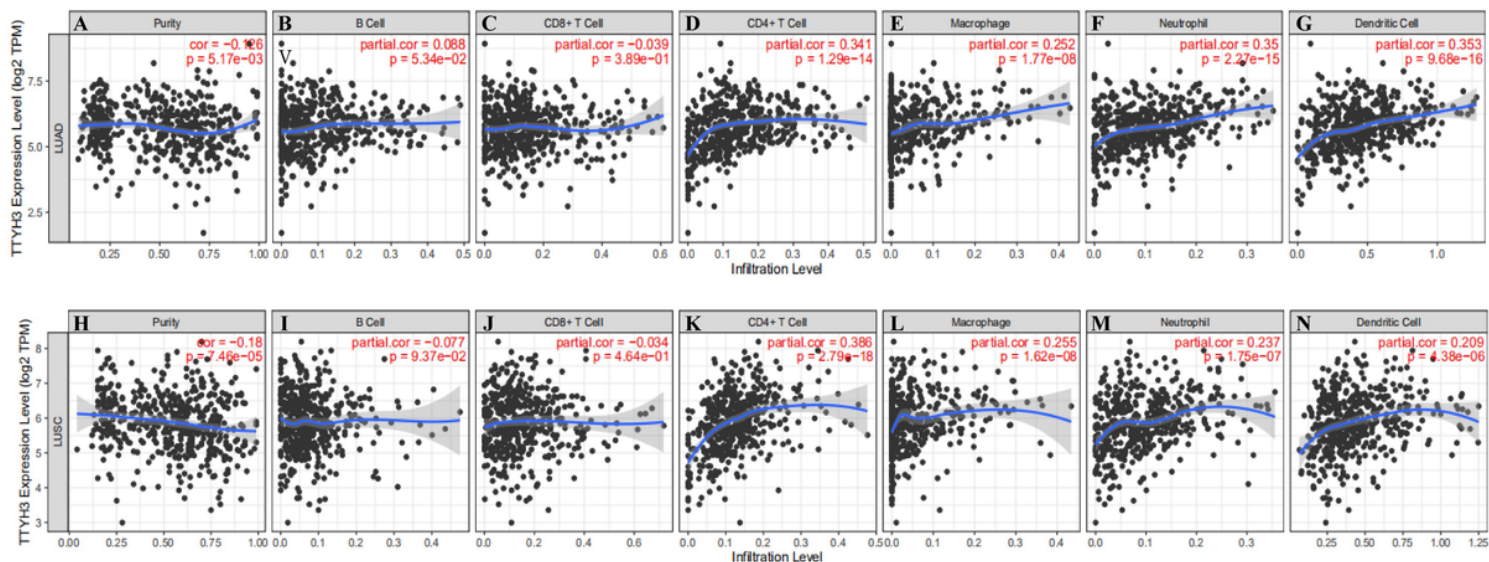


Figure 8

Correlation between TTYH3 and immune cells in LUAD/LUSC. (A-G) TIMER showed that TTYH3 was associated with tumor purity and immune infiltration levels in LUAD including B cell, CD8⁺ T cell, CD8⁺ T cell, Macrophage, Neutrophil and Dendritic cell. (H-N) The same outcomes detected in LUSC. Abbreviation: LUAD, lung adenocarcinoma; LUSC, lung squamous cell carcinoma.

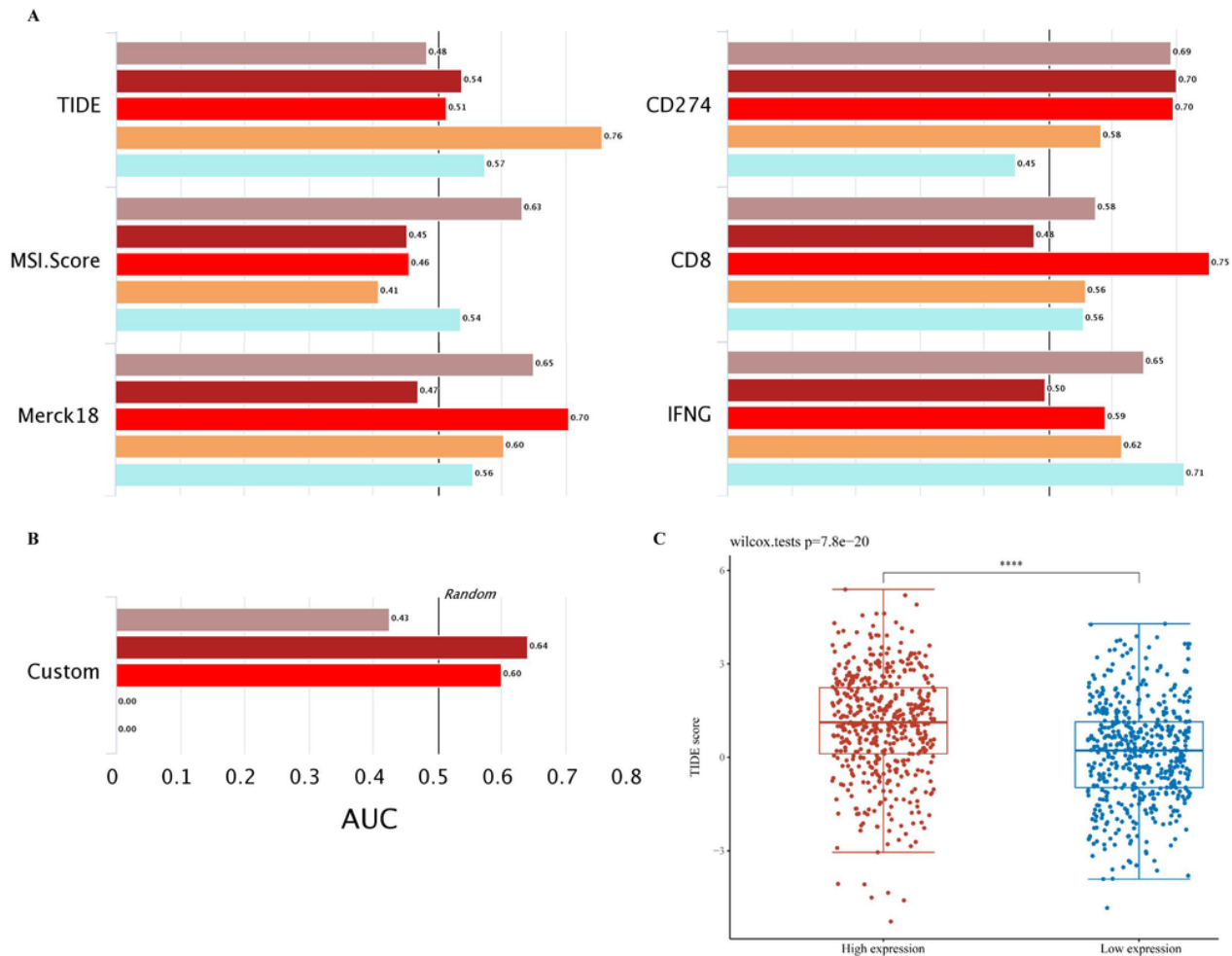


Figure 9

TTYH3 owned a predictive value for immunotherapy response in lung cancer. (A) The accuracy of TTYH3 was evaluated in comparison with other published biomarkers including TIDE score, CD274 (PD-L1), MSI Score (microsatellite instability score), CD8, Merck18 and IFNG (Interferon-gamma) in lung cancer. (B) Custom represented the test biomarker is composed of genes with consistent evidence on cancer immune evasion genes including SERPINB9, TGFB1, PDL1, FAP, VEGFA, IFNG and ANGPT2. These genes were weighted by their reported direction of mediating anticancer immune response. The area under receiver operating characteristic curve (AUC) is applied to evaluate the prediction performance of the test biomarker on the ICB response status and the different colors meant different study cohorts. TTYH3' AUC were visualized by bar plots and when it's greater than 0.5, suggests TTYH3 to be a robust predictive biomarker. (C) TIDE score analysis of TTYH3 expression difference. The red dots represent lung cancer samples with high TTYH3 expression and the blue dots represent low TTYH3 expression. There were 507 lung cancer samples in each group. The significance of the two groups was tested by Wilcox, **** p < 0.0001.

This is a list of supplementary files associated with this preprint. Click to download.

- [TableS1.docx](#)